Chemical Science

ROYAL SOCIETY OF CHEMISTRY

EDGE ARTICLE

View Article Online
View Journal | View Issue

Cite this: *Chem. Sci.*, 2020, **11**, 8145

All publication charges for this article have been paid for by the Royal Society of Chemistry

Received 10th June 2020
Accepted 17th July 2020

DOI: 10.1039/d0sc03223a

rsc.li/chemical-science

An atropisomeric M_2L_4 cage mixture displaying guest-induced convergence and strong guest emission in water†

Takahiro Tsutsui,‡[a] Lorenzo Catti,‡[b] Kenji Yoza[c] and Michito Yoshizawa*[a]

Introduction of atropisomeric axes into a bent bispyridine ligand leads to the quantitative formation of a complex mixture of atropisomeric M_2L_4 cages upon treatment with metal ions. Whereas the isomer ratio of the obtained cage mixture, consisting of up to 42 isomers, is insensitive to temperature and solvent, the quantitative convergence from the mixture to a single isomer is accomplished upon encapsulation of a large spherical guest, namely fullerene C_{60}. The observed isomerization with other guests depends largely on their size and shape (*e.g.*, <10 and 82% convergence with planar triphenylene and bowl-shaped corannulene guests, respectively). Besides the unusual guest-induced convergence, the present cage mixture displays the strongest guest emission (Φ_F = 68%) among previously reported M_nL_m cages and capsules, upon encapsulation of a BODIPY dye in water.

Introduction

Biological assemblies such as viral capsids and ferritins display well-organized, spherical nanoarchitectures yet consist of unsymmetrical protein subunits bearing flexible moieties before assembly (Fig. 1a).[1] On the other hand, synthetic chemists are apt to design highly symmetrical subunits with sufficient conformational rigidity to precisely construct spherical nanostructures through hydrogen bonding[2] and coordination-driven self-assemblies,[3] *e.g.*, a spherical M_2L_4 cage (Fig. 1b).[4] The cavity size and properties of such artificial assemblies are also highly controllable by the use of the well-designed components.[5] In contrast, desymmetrized, synthetic subunits with one or more isomerizable moieties give rise to a complex mixture of product isomers *via* self-assembly (*e.g.*, Fig. 1c). So far, no rational method has been reported to converge such complex, artificial mixtures (so-called dynamic combinatorial libraries)[6] into a single, three-dimensional isomer.

Herein we report the design and synthesis of bent bispyridine ligand **1** with *two atropisomeric axes* (Fig. 2a). Treatment of the isomerizable and desymmetrized ligands with metal ions leads to the quantitative formation of a complex mixture of atropisomeric M_2L_4 cages **2** (Fig. 2b). Although the isomer ratio of the resultant cages is insensitive to temperature and solvent, the selective and quantitative convergences from the complex mixture to a single isomer are demonstrated upon encapsulation of spherical corannulene dimer and fullerene C_{60}, respectively. In addition, the present cage mixture displays the strongest guest emission (Φ_F = 68%), as compared to previously reported M_nL_m cages and capsules,[7] upon encapsulation of a fluorescent BODIPY dye.

As the simplest model, we chose a highly symmetrical M_2L_4 structure to examine its desymmetrization and convergence. It has been established that bent bispyridine ligands with a virtual C_{2v} symmetry generate M_2L_4 cages or capsules as a single isomer upon complexation with metal ions (Fig. 1b).[4] Their host abilities have been widely investigated by many groups so far.[8,9] Thus we introduced atropisomeric axes[10] into the ligand and

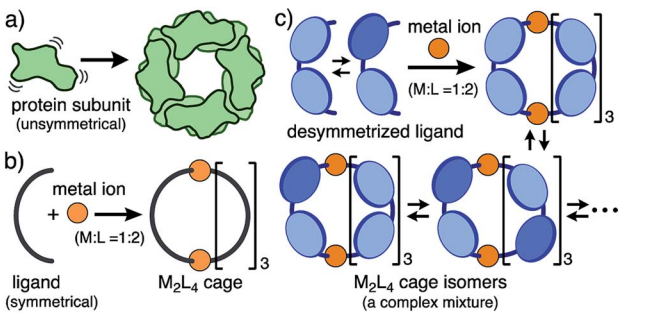

Fig. 1 Schematic representation of the self-assemblies of (a) a biological nanostructure, (b) an M_2L_4 cage from symmetrical ligands and metal ions, and (c) a complex mixture of M_2L_4 cage isomers from desymmetrized ligands and metal ions studied herein.

[a]*Laboratory for Chemistry and Life Science, Institute of Innovative Research, Tokyo Institute of Technology, 4259 Nagatsuta, Midori-ku, Yokohama 226-8503, Japan. E-mail: yoshizawa.m.ac@m.titech.ac.jp*

[b]*WPI Nano Life Science Institute, Kanazawa University, Kakuma-machi, Kanazawa 920-1192, Japan*

[c]*Bruker AXS, 3-9 Moriya-cho, Kanagawa-ku, Yokohama 221-0022, Japan*

† Electronic supplementary information (ESI) available. CCDC 1907426. For ESI and crystallographic data in CIF or other electronic format see DOI: 10.1039/d0sc03223a

‡ These authors contributed equally.

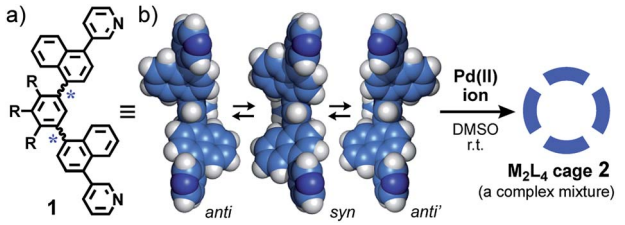

Fig. 2 Schematic representation of (a) bispyridine ligand **1** (R = $-OCH_2CH_2OCH_3$) and, (b) the optimized structures of the atropisomers in equilibrium (DFT calculation, B3LYP/6-31* level, R = $-OCH_3$) and the formation of M_2L_4 cage **2** as a complex isomeric mixture.

designed 1,4-naphthylene-embedded, bent ligand **1** (Fig. 2a). The new bispyridine ligand adopts three atropisomers owing to hindered rotation around the phenyl–naphthyl bonds so that the corresponding atropisomeric M_2L_4 cage, possessing a spherical hydrophobic cavity (~1 nm in diameter), is anticipated to be present as an equilibrium mixture of up to 42 isomers (Fig. 3).

Results and discussion

Formation of a complex mixture of M_2L_4 cages

First we observed the quantitative formation of a complex mixture of M_2L_4 cage **2** isomers by mixing atropisomeric ligand **1**, $PdCl_2(DMSO)_2$, and $AgNO_3$ (in a 2 : 1 : 2 ratio) in DMSO-d_6 for 1 h at room temperature (Fig. 2).[11,12a] As expected, the ^{1}H NMR spectrum of the product mixture showed complicated and broadened, aromatic signals in the range of 9.7 to 6.6 ppm, in contrast to the simple and sharp signals observed for free ligand **1** (Fig. 4a and b). The ^{1}H DOSY NMR spectrum revealed that these proton signals have the same diffusion constant ($D = 1.2 \times 10^{-10}$ m^2 s^{-1}; Fig. 4c),[12b] indicating the existence of Pd(II)-linked cage **2** as an isomeric mixture in equilibrium. The exclusive formation of M_2L_4 assemblies **2** was unambiguously confirmed by ESI-TOF MS analysis: prominent peaks were

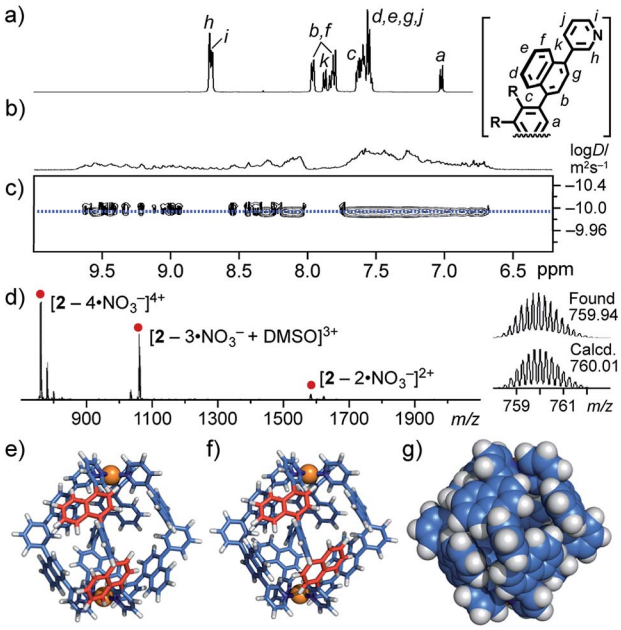

Fig. 4 ^{1}H NMR spectra (500 MHz, DMSO-d_6, r.t.) of (a) ligand **1** and (b) a complex mixture of cage isomers **2**. (c) ^{1}H DOSY NMR (500 MHz, DMSO-d_6, 298 K) and (d) ESI-TOF MS (DMSO, r.t.) spectra of isomers **2**. Optimized structures of **2**: (e) an all-*syn* isomer and (f and g) an all-*anti* isomer (substituents and counterions are omitted for clarity).

observed at *m*/*z* 759.9, 1033.9, and 1582.3, assignable to the $[\mathbf{2} - n\cdot NO_3^-]^{n+}$ species (n = 4, 3, and 2, respectively; Fig. 4d). In a manner similar to **2**, Pt(II)-analogue **2′** was formed quantitatively and its M_2L_4 structure was confirmed by NMR and MS analyses.[11] The existence of various isomers of **2′** was also established by the complicated and broadened ^{1}H NMR signals (Fig. S23†).

The theoretical calculation of cage **2** indicated that differences in energy are relatively small among representative isomers (ΔE < 1.8 kcal mol^{-1}; *e.g.*, Fig. 4e, f and S22†),[11] supporting the complex signals observed in the ^{1}H NMR spectrum

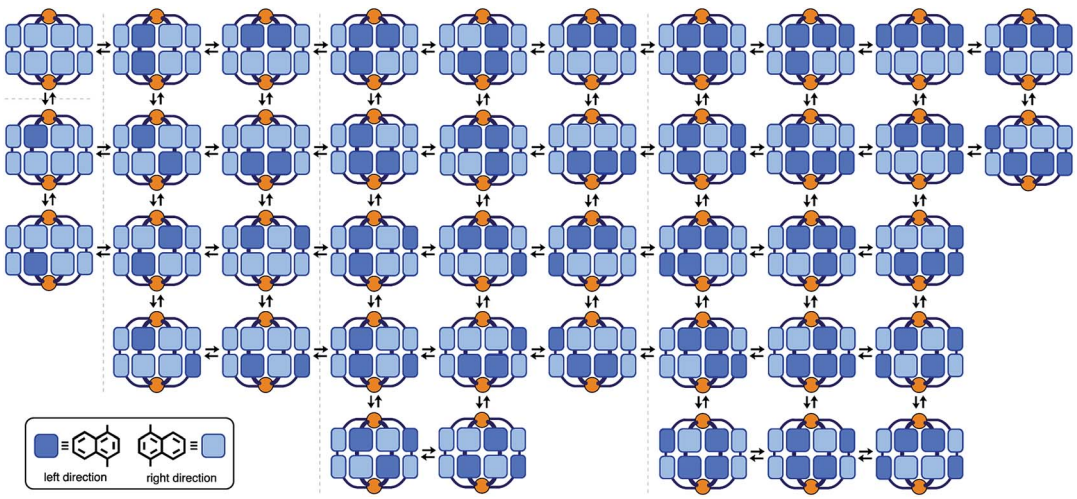

Fig. 3 Schematic representation of the possible 42 isomers of M_2L_4 cage **2**. These isomers are in equilibrium in solution.

(Fig. 4b). The optimized structure of **2** (*e.g.*, an all-*anti* isomer, Fig. 4g) clarified that the spherical cavity (~580 Å^3) is surrounded by eight naphthalene panels and the cavity diameter is 1.3 nm. Although the cavity shape and size are almost identical to those of anthracene-based M_2L_4 capsule **3** reported previously (Fig. S1†),[9,11] the bent polyaromatic ligands of **2** are proximate to each other yet unstacked.

Guest-induced convergence to a single isomer

Whereas the isomer ratio of cage **2** remained intact even upon changing the solvent (*e.g.*, CD_3CN, CD_3OD, and D_2O) and temperature (*e.g.*, −10 to 110 °C), guest encapsulation allowed the complex mixture to convert into a single isomer in water. When a simple planar and hydrophobic guest, triphenylene (**Tp**; excess), was mixed with a D_2O solution of **2** (0.6 mM) at room temperature for 1 h (Fig. 5a), the ^{1}H NMR signals of **2** changed from completely broad[13] to slightly sharp (Fig. 5b and c), due to the quantitative incorporation of the guests (2 equiv.) into the host cavity through the hydrophobic effect.[14] The NMR signals were unchanged even at elevated temperature (*e.g.*, 80 °C). The ESI-TOF MS analysis of the product clearly supported the formation of 1 : 2 host–guest complex **2**·(**Tp**)$_2$ (Fig. S27c†). This result indicated the possibility of wide-ranging host abilities of **2** in water and selective isomerization of **2** through an appropriate guest stimulus.[15]

Next, the treatment of small spherical adamantane (**Ad**) and bowl-shaped corannulene (**Cor**) with cage mixture **2** gave rise to host–guest complexes **2**·**Ad** and **2**·(**Cor**)$_2$ in a quantitative manner, respectively, under the same aqueous conditions (Fig. 5a).[15] Interestingly, the resultant ^{1}H NMR spectra revealed further conversion from the complex mixtures to a single isomer upon binding of the sterically demanding guests, whose shapes are similar to the spherical cavity of **2**. The percentages of the generated, major host isomer accommodating **Ad** and (**Cor**)$_2$ guests were estimated to be 75 and 82, respectively (Fig. 5d and e), on the basis of the reference proton signal of the methoxy groups of **2** around 2.96–2.83 ppm. The aliphatic proton signals of bound **Ad** appeared around −0.7 ppm, due to the aromatic shielding effect of **2** (Fig. S28a†). The eleven aromatic signals were clearly observed in the ^{1}H NMR spectrum of **2**·(**Cor**)$_2$ (Fig. 5e). Noteworthy, a similar ^{1}H NMR spectrum was obtained from a mixture of cage **2′**, which is an analogue of **2** with Pt(II) ions, and excess **Cor** in D_2O at room temperature for 7 h (Fig. S30†).[11] The finding revealed that the naphthalene panels embedded in the spherical framework of **2** can flip even at ambient temperature, because the bonds between the Pt(II) hinges and the pyridyl groups are fixed under these conditions.

The quantitative conversion of the mixture into a single isomer was accomplished upon incorporation of spherical fullerene C_{60} (C_{60}) into cage **2**. Mixing of cage **2** with excess C_{60} in D_2O at 100 °C for 24 h yielded 1 : 1 host–guest complex **2**·C_{60} exclusively. Intense ESI-TOF MS peaks at m/z = 940.2 and 1274.2 were assignable to $[2\cdot C_{60} - n\cdot NO_3^-]^{n+}$ species (n = 4 and 3; Fig. 5g). Notably, the ^{1}H NMR spectrum of **2**·C_{60} exhibited only eleven signals in the aromatic region, indicating the presence of a single isomer (~100% selectivity; Fig. 5f). In the ^{13}C NMR spectrum of **2**·C_{60}, a single signal for the C_{60} guest was observed at 140.1 ppm (Fig. S32†), in a manner similar to that of the previous C_{60}-incorporated M_2L_4 capsule (141.2 ppm).[9a] The broadened, new UV-visible absorption bands derived from the guest were also found around 400–730 nm (Fig. S36†).[16] In short, these results revealed that the "atropisomeric" dynamic combinatorial library[6] of cage **2** can be strictly controlled by its size (volume) and shape complementary guest molecules.

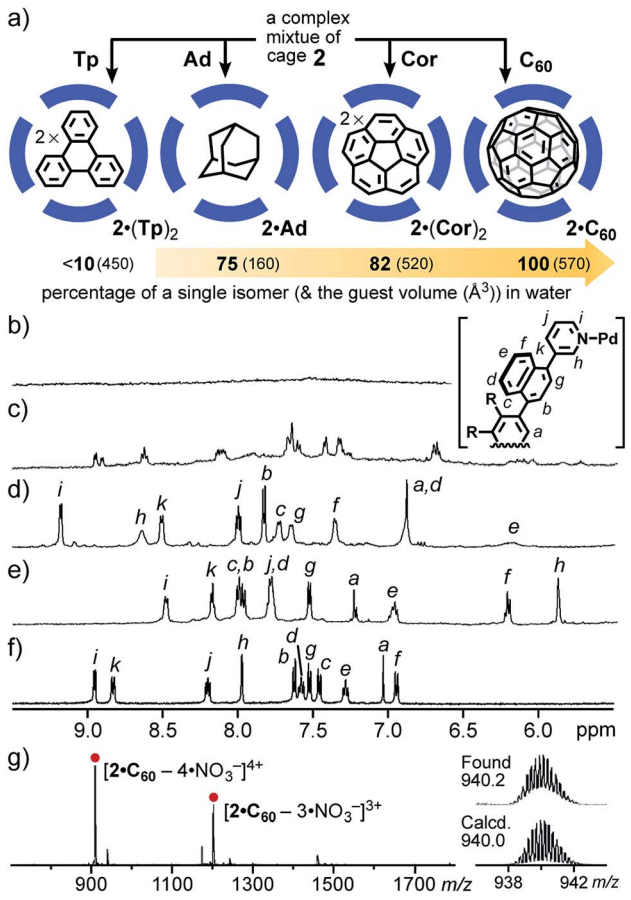

Fig. 5 (a) Schematic representation of the guest-induced convergence of a complex mixture of **2**. ^{1}H NMR spectra (500 MHz, D_2O, r.t.) of (b) cage **2**, (c) **2**·(**Tp**)$_2$, (d) **2**·**Ad**, (e) **2**·(**Cor**)$_2$, and (f) **2**·C_{60}. (g) ESI-TOF MS spectrum (H_2O) of **2**·C_{60} and the expansion and simulation of the $[2\cdot C_{60} - 4\cdot NO_3^-]^{4+}$ signals.

Crystallographic analysis of the single isomer

The direction of the eight naphthalene panels on **2**·C_{60} was eventually determined by X-ray crystallographic and theoretical analyses.[11,17,18] As we expected, the crystal structure showed that one molecule of C_{60} is fully captured by the cage-shaped M_2L_4 framework of **2** (Fig. 6a). Remarkably, all the bent bispyridine ligands adopted a *syn* conformation and aligned roundly in the same direction (Fig. 6b), most probably to avoid the steric repulsion between the naphthalene panels of the adjacent ligands. The π-stacking interactions between C_{60} and the naphthalene panels were observed at eight positions (d = 3.2–3.4 Å in interplanar distance; Fig. S38†). The theoretical

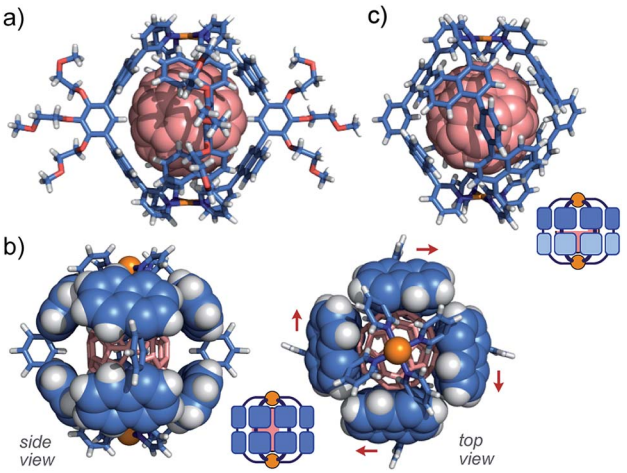

Fig. 6 X-ray crystal structure of $2\cdot C_{60}$ (all-*syn* isomer): (a) space-filling representation for C_{60} and (b) space-filling representation for the naphthalene panels (the substituents are replaced by H atoms for clarity). (c) Optimized structure of $2\cdot C_{60}$ (all-*anti* isomer, R = –H).

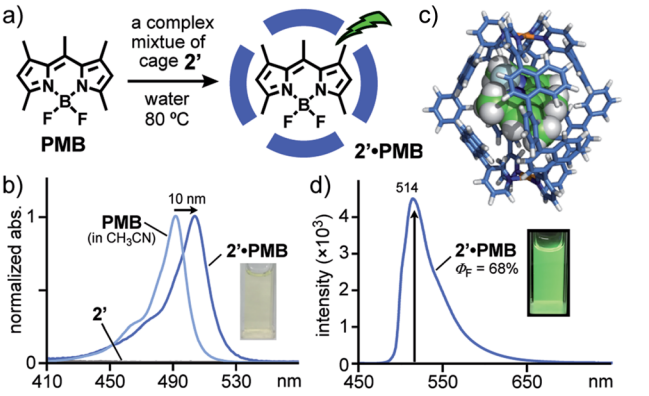

Fig. 7 (a) Schematic representation of the formation of highly emissive host–guest complex $2'\cdot$**PMB**. (b) UV-visible spectra and photograph (H_2O, r.t.) of $2'\cdot$**PMB**, $2'$, and **PMB** (in CH_3CN). (c) Optimized structure of $2'\cdot$**PMB** (R = –H, all-*syn* isomer). (d) Fluorescence spectrum (H_2O, r.t., 80 μM based on $2'$, λ_{ex} = 500 nm) of $2'\cdot$**PMB** and its photograph (λ_{ex} = 365 nm).

calculations of $2\cdot C_{60}$ (R = –H) on the basis of the present crystal structure indicated that the energy of the all-*syn* isomer (Fig. 6a) is 10.6 kcal mol^{-1} lower than that of an all-*anti* isomer (Fig. 6c) in the gas phase. The cage framework possesses four small openings (approximately 4 × 5 $Å^2$) between the polyaromatic ligands, in contrast to previous M_2L_4 capsule **3** with an anthracene-based, closed shell.[9] Preliminary host–guest studies showed the selective binding of one molecule of functionalized fullerenes (*e.g.*, diethyl malonate-derivatized C_{60}) by the present cage in water (Fig. S40†).[11]

Strong emission of an encapsulated BODIPY derivative

Finally, we encountered that naphthalene-based Pt(II)-cage $2'$ displays very strong guest emission upon encapsulation of a BODIPY dye in water.[19] After stirring a mixture of cage $2'$ and water-insoluble, pentamethyl boron-dipyrromethene **PMB** (9 equiv.) in D_2O at 80 °C for 1.5 h (Fig. 7a), the formation of 1 : 1 host–guest complex $2'\cdot$**PMB** was evidenced by NMR, MS, and UV-visible analyses. The obtained, broad ^{1}H NMR signals indicated the existence of a complex isomeric mixture including the guest dye (Fig. S41a†). The 1 : 1 host–guest ratio of the product was confirmed by the ESI-TOF MS spectrum, which shows clear MS peaks for $[2'\cdot\mathbf{PMB} - n\cdot NO_3^-]^{n+}$ species (n = 4, 3; Fig. S41b†). The UV-visible spectrum of the pale yellow solution of $2'\cdot$**PMB** in water showed new absorption bands in the range of 410–550 nm, derived from encapsulated **PMB** (Fig. 7b). The observed bands were slightly red-shifted ($\Delta\lambda$ = 10 nm) with respect to those of free **PMB** in CH_3CN and their intensity indicated the encapsulation efficiency being ~25%. The optimized structure of $2'\cdot$**PMB** (R = –H) suggested that a slightly bent **PMB** framework is fully accommodated in the polyaromatic shell of $2'$ (Fig. 7c).[11]

Host–guest complexes featuring high emissivity in water have attracted considerable attention related to biomolecular sensors. However, the majority of coordination cages and capsules disturb guest emission upon encapsulation, owing to the heavy metal effect.[3–6] Our previous studies exceptionally demonstrated strong fluorescence (λ_{max} = 535 nm, Φ_F = 48%) from a 1 : 1 host–guest complex, composed of anthracene-based capsule **3** and **PMB** in water.[7c] Notably, the aqueous solution of $2'\cdot$**PMB** emitted much stronger green fluorescence with a quantum yield of 68% at λ_{max} = 514 nm, upon irradiation at 500 nm (Fig. 7d). The band shape and maximum wavelength are similar to those of free **PMB** in ethanol (λ_{max} = 522 nm, Φ_F = 78%). To the best of our knowledge, this represents the strongest guest emission in coordination host compounds reported so far.[7] As compared to capsule **3** with a relatively rigid cavity,[9] the flexible naphthalene-based cavity of $2'$ is able to adjust to the shape of the bulky **PMB** guest (Fig. 7c), which reduces the steric host–guest repulsion. Once the cage encapsulates the guest, the flexibility of the naphthalene panels is largely suppressed due to the efficient host–guest interactions. These effects might suppress emission quenching processes, observed in the case of $3\cdot$**PMB**, to a large degree ($\Delta\Phi_F$ = +20%).[19]

Conclusions

We have challenged the perfect conversion of a complex mixture of atropisomeric M_2L_4 cages into a single isomer by an external stimulus. The cage mixture including up to 42 isomers was generated upon incorporation of two atropisomeric axes into the bent bispyridine ligands of a common and highly symmetrical M_2L_4 structure. Unusual convergence of the mixed isomers was demonstrated upon encapsulation of guest molecules. Particularly, the encapsulation of a fullerene guest led to the quantitative formation of a single isomer, due to its size and shape complementarity to the spherical host cavity. Thus, the present system can be regarded as a novel dynamic combinatorial library capable of incorporating large guests up to 1 nm. The isomer structure (all-*syn*) of the M_2L_4 cage was fully characterized by NMR, MS, UV-visible, X-ray crystallographic, and theoretical analyses. As an additional host function, the cage

mixture encapsulated a fluorescent BODIPY dye and the resultant 1 : 1 host–guest complex exhibited intense guest emission (Φ_F = ~70%) in water. We believe that the present study is a small yet first "synthetic" step to approach large and well-organized, biological capsules, composed of multiple unsymmetrical subunits, *in vitro*.

Conflicts of interest

There are no conflicts to declare.

Acknowledgements

This work was supported by JSPS KAKENHI (Grant No. JP18H01990/JP19H04566) and "Support for Tokyotech Advanced Researchers (STAR)". We thank Prof. Munetaka Akita and Dr Naoki Noto for helpful discussion and L. C. thanks the JSPS and Humboldt Postdoctoral Fellowship.

Notes and references

1 M. G. Mateu, *Arch. Biochem. Biophys.*, 2013, **531**, 65–79.
2 Representative examples: (*a*) R. Meissner, J. d. Mendoza and J. Rebek Jr, *Science*, 1995, **270**, 1485–1488; (*b*) L. R. MacGillivray and J. L. Atwood, *Nature*, 1997, **389**, 469–472; (*c*) J. Rebek Jr, *Acc. Chem. Res.*, 1999, **32**, 278–286.
3 Representative examples: (*a*) M. Tominaga, K. Suzuki, M. Kawano, T. Kusukawa, T. Ozeki, S. Sakamoto, K. Yamaguchi and M. Fujita, *Angew. Chem., Int. Ed.*, 2004, **43**, 5621–5625; (*b*) Q.-F. Sun, J. Iwasa, D. Ogawa, Y. Ishido, S. Sato, T. Ozeki, Y. Sei, K. Yamaguchi and M. Fujita, *Science*, 2010, **328**, 1144–1147; (*c*) D. Fujita, Y. Ueda, S. Sato, N. Mizuno, T. Kumasaka and M. Fujita, *Nature*, 2016, **540**, 563–566.
4 (*a*) N. B. Debata, D. Tripathy and D. K. Chand, *Coord. Chem. Rev.*, 2012, **256**, 1831–1945; (*b*) A. Schmidt, A. Casini and F. E. Kühn, *Coord. Chem. Rev.*, 2014, **275**, 19–36.
5 For recent reviews: (*a*) K. Harris, D. Fujita and M. Fujita, *Chem. Commun.*, 2013, **49**, 6703–6712; (*b*) T. R. Cook and P. J. Stang, *Chem. Rev.*, 2015, **115**, 7001–7045; (*c*) C. J. Brown, F. D. Toste, R. G. Bergman and K. N. Raymond, *Chem. Rev.*, 2015, **115**, 3012–3035; (*d*) M. Yoshizawa and M. Yamashina, *Chem. Lett.*, 2017, **46**, 163–171; (*e*) R. A. S. Vasdev, D. Preston and J. D. Crowley, *Chem.–Asian J.*, 2017, **12**, 2513–2523; (*f*) L.-J. Chen, H.-B. Yang and M. Shionoya, *Chem. Soc. Rev.*, 2017, **46**, 2555–2576; (*g*) S. Chakraborty and G. R. Newkome, *Chem. Soc. Rev.*, 2018, **47**, 3991–4016; (*h*) I. Sinha and P. S. Mukherjee, *Inorg. Chem.*, 2018, **57**, 4205–4221; (*i*) F. J. Rizzuto, L. K. S. von Krbek and J. R. Nitschke, *Nat. Rev. Chem.*, 2019, **3**, 204–222; (*j*) M. Yoshizawa and L. Catti, *Acc. Chem. Res.*, 2019, **52**, 2392–2404; (*k*) H. Sepehrpour, W. Fu, Y. Sun and P. J. Stang, *J. Am. Chem. Soc.*, 2019, **141**, 14005–14020; (*l*) J. E. M. Lewis and J. D. Crowley, *ChemPlusChem*, 2020, **85**, 815–827.
6 In contrast to previously reported, dynamic combinatorial libraries, the present library possesses an isolated cavity capable of encapsulating large guests up to 1 nm in water: (*a*) J.-M. Lehn, *Chem.–Eur. J.*, 1999, **5**, 2455–2463; (*b*) G. R. L. Cousins, S. A. Poulsen and J. K. M. Sanders, *Curr. Opin. Chem. Biol.*, 2000, **4**, 270–279; (*c*) J.-M. Lehn and A. V. Eliseev, *Science*, 2001, **291**, 2331–2332.
7 Fluorescent host–guest complexes based on coordination hosts (up to Φ_F = 48%): (*a*) K. Ono, J. K. Klosterman, M. Yoshizawa, K. Sekiguchi, T. Tahara and M. Fujita, *J. Am. Chem. Soc.*, 2009, **131**, 12526–12527; (*b*) P. P. Neelakandan, A. Jiménez and J. R. Nitschke, *Chem. Sci.*, 2014, **5**, 908–915; (*c*) M. Yamashina, M. Sartin, Y. Sei, M. Akita, S. Takeuchi, T. Tahara and M. Yoshizawa, *J. Am. Chem. Soc.*, 2015, **137**, 9266–9269; (*d*) D. R. Martir, A. Pizzolante, D. Escudero, D. Jacquemin, S. L. Warriner and E. Zysman-Colman, *ACS Appl. Energy Mater.*, 2018, **1**, 2971–2978; (*e*) T. Tsutsui, S. Kusaba, M. Yamashina, M. Akita and M. Yoshizawa, *Chem.–Eur. J.*, 2019, **25**, 4320–4324; (*f*) H. Dobashi, L. Catti, Y. Tanaka, M. Akita and M. Yoshizawa, *Angew. Chem., Int. Ed.*, 2020, **59**, 11881–11885.
8 Representative examples: (*a*) D. A. McMorran and P. J. Steel, *Angew. Chem., Int. Ed.*, 1998, **37**, 3295–3297; (*b*) L. J. Barbour, G. W. Orr and J. L. Atwood, *Nature*, 1998, **393**, 671–673; (*c*) J. E. M. Lewis, E. L. Gavey, S. A. Cameron and J. D. Crowley, *Chem. Sci.*, 2012, **3**, 778–784; (*d*) G. H. Clever, W. Kawamura, S. Tashiro, M. Shiro and M. Shionoya, *Angew. Chem., Int. Ed.*, 2012, **51**, 2606–2609; (*e*) M. Han, R. Michel, B. He, Y.-S. Chen, D. Stalke, M. John and G. H. Clever, *Angew. Chem., Int. Ed.*, 2013, **52**, 1319–1323; (*f*) D. P. August, G. S. Nichol and P. J. Lusby, *Angew. Chem., Int. Ed.*, 2016, **55**, 15022–15026; (*g*) V. Martí-Centelles, A. L. Lawrence and P. J. Lusby, *J. Am. Chem. Soc.*, 2018, **140**, 2862–2868.
9 (*a*) N. Kishi, Z. Li, K. Yoza, M. Akita and M. Yoshizawa, *J. Am. Chem. Soc.*, 2011, **133**, 11438–11441; (*b*) S. Matsuno, M. Yamashina, Y. Sei, M. Akita, A. Kuzume, K. Yamamoto and M. Yoshizawa, *Nat. Commun.*, 2017, **8**, 749; (*c*) M. Yamashina, M. Akita, T. Hasegawa, S. Hayashi and M. Yoshizawa, *Sci. Adv.*, 2017, **3**, e1701126; (*d*) M. Yamashina, S. Kusaba, M. Akita, T. Kikuchi and M. Yoshizawa, *Nat. Commun.*, 2018, **9**, 4227; (*e*) M. Yamashina, T. Tsutsui, Y. Sei, M. Akita and M. Yoshizawa, *Sci. Adv.*, 2019, **5**, eaav3179; (*f*) K. Niki, T. Tsutsui, M. Yamashina, M. Akita and M. Yoshizawa, *Angew. Chem., Int. Ed.*, 2020, **59**, 10489–10492; (*g*) N. Kishida, K. Matsumoto, Y. Tanaka, M. Akita, H. Sakurai and M. Yoshizawa, *J. Am. Chem. Soc.*, 2020, **142**, 9599–9603.
10 Atropisomeric cages: (*a*) T. Kamada, N. Aratani, T. Ikeda, N. Shibata, Y. Higuchi, A. Wakamiya, S. Yamaguchi, K. S. Kim, Z. S. Yoon, D. Kim and A. Osuka, *J. Am. Chem. Soc.*, 2006, **128**, 7670–7678; (*b*) S. Arai, D. Niwa, H. Nishide and S. Takeoka, *Org. Lett.*, 2007, **9**, 17–20; (*c*) A. Suzuki, K. Kondo, M. Akita and M. Yoshizawa, *Angew. Chem., Int. Ed.*, 2013, **52**, 8120–8123.
11 See the ESI.† The geometry optimizations of the cages and host–guest complexes were performed with molecular mechanics (MM) calculations (Forcite module, Materials Studio, version 5.5.3). Particularly, the optimized

structures and energies of all-*syn*/*anti* $\mathbf{2}\cdot\mathbf{C_{60}}$ isomers were calculated on the basis of the crystal structure.

12 (*a*) Ligand **1** was synthesized in three steps using 3-pyridineboronic acid pinacol ester, 1,4-dibromonaphthalene, and 1,5-dibromo-2,3,4-tri(2-methoxyethoxy)-benzene;[11] (*b*) The diffusion constant indicates the product size (outer diameter) being approximately 2 nm.

13 In the ^{1}H NMR spectrum, the signals of a mixture of **2** in D_2O (Fig. 5b) are much broader than those in DMSO-d_6 (Fig. 4b), because of strong interactions between the naphthalene-based bispyridine ligands, induced by the hydrophobic effect.

14 The ESI-TOF MS analysis of the products elucidated the host–guest ratios (except for the labile $\mathbf{2}\cdot\mathbf{Ad}$ complex under MS conditions). In addition, the ratios were also estimated by the ^{1}H NMR integrations of the products after disassembly in DMSO-d_6 (at 80 °C for 1 h under high dilution conditions).

15 The guest-induced isomerization of coordination cage frameworks is uncommon, whereas there have been several reports on guest-induced structural changes of coordination cages: (*a*) M. Scherer, D. L. Caulder, D. W. Johnson and K. N. Raymond, *Angew. Chem., Int. Ed.*, 1999, **38**, 1588–1592; (*b*) S. Hiraoka and M. Fujita, *J. Am. Chem. Soc.*, 1999, **121**, 10239–10240; (*c*) K. Umemoto, K. Yamaguchi and M. Fujita, *J. Am. Chem. Soc.*, 2000, **122**, 7150–7151; (*d*) D. M. Wood, W. Meng, T. K. Ronson, A. R. Stefankiewicz, J. K. M. Sanders and J. R. Nitschke, *Angew. Chem., Int. Ed.*, 2015, **54**, 3988–3992; (*e*) M. Kieffer, R. A. Bilbeisi, J. D. Thoburn, J. K. Clegg and J. R. Nitschke, *Angew. Chem., Int. Ed.*, 2020, **59**, 11369–11373.

16 The absorption bands of the electron-deficient $\mathbf{C_{60}}$ guest are sensitive to the polyaromatic host framework due to the efficient host–guest interactions.[7f] The electron-donating properties of the host framework are decreased by the replacement of the anthracene panels with naphthalene panels so that large blue shifts of the guest absorption bands were observed in $\mathbf{2}\cdot\mathbf{C_{60}}$ as compared with an anthracene-based host–guest analogue.[9a]

17 The brown block crystals of $\mathbf{2}\cdot\mathbf{C_{60}}$ were obtained by slow concentration of a 2 : 1 acetonitrile/water solution of $\mathbf{2}\cdot\mathbf{C_{60}}$ over 3 weeks at room temperature. Whereas there have been many reports on the successful X-ray crystallographic analysis of M_2L_4 hosts,[4,8,9] reports on host–guest complexes including one $\mathbf{C_{60}}$ guest are still rare.[18]

18 (*a*) C. García-Simón, M. Costas and X. Ribas, *Chem. Soc. Rev.*, 2016, **45**, 40–62; (*b*) B. Chen, J. J. Holstein, S. Horiuchi, W. G. Hiller and G. H. Clever, *J. Am. Chem. Soc.*, 2019, **141**, 8907–8913.

19 Cage **2′** was chosen for this study due to the pronounced heavy-atom fluorescence quenching effect of the Pd(II)-analogue. A detailed study of the emission dynamics has been performed with $\mathbf{3}\cdot\mathbf{PMB}$, using fluorescence lifetime and femtosecond transient absorption measurements.[7c]